The Plant Cell, Vol. 25: 3347–3359, September 2013, www.plantcell.org

The Ubiquitin Receptor DA1 Interacts with the E3 Ubiquitin Ligase DA2 to Regulate Seed and Organ Size in *Arabidopsis*[C][W]

Tian Xia,[a,c,1] Na Li,[a,1] Jack Dumenil,[b,1] Jie Li,[a] Andrei Kamenski,[d] Michael W. Bevan,[b] Fan Gao,[a,c] and Yunhai Li[a,2]

[a] State Key Laboratory of Plant Cell and Chromosome Engineering, Institute of Genetics and Developmental Biology, Chinese Academy of Sciences, Beijing 100101, China
[b] Department of Cell and Developmental Biology, John Innes Centre, Norwich NR4 7UH, United Kingdom
[c] University of Chinese Academy of Sciences, Beijing 100039, China
[d] Department of Biology, University of York, York YO10 5DD, United Kingdom

ORCID ID: 0000-0002-0025-4444 (Y.L.).

Seed size in higher plants is determined by the coordinated growth of the embryo, endosperm, and maternal tissue. Several factors that act maternally to regulate seed size have been identified, such as AUXIN RESPONSE FACTOR2, APETALA2, KLUH, and DA1, but the genetic and molecular mechanisms of these factors in seed size control are almost totally unknown. We previously demonstrated that the ubiquitin receptor DA1 acts synergistically with the E3 ubiquitin ligase ENHANCER1 OF DA1 (EOD1)/BIG BROTHER to regulate the final size of seeds in *Arabidopsis thaliana*. Here, we describe another RING-type protein with E3 ubiquitin ligase activity, encoded by *DA2*, which regulates seed size by restricting cell proliferation in the maternal integuments of developing seeds. The *da2-1* mutant forms large seeds, while overexpression of *DA2* decreases seed size of wild-type plants. Overexpression of rice (*Oryza sativa*) *GRAIN WIDTH AND WEIGHT2*, a homolog of *DA2*, restricts seed growth in *Arabidopsis*. Genetic analyses show that *DA2* functions synergistically with *DA1* to regulate seed size, but does so independently of *EOD1*. Further results reveal that DA2 interacts physically with DA1 in vitro and in vivo. Therefore, our findings define the genetic and molecular mechanisms of three ubiquitin-related proteins DA1, DA2, and EOD1 in seed size control and indicate that they are promising targets for crop improvement.

INTRODUCTION

Seed size in higher plants is central to many aspects of evolutionary fitness and is also an important trait for agricultural purposes (Alonso-Blanco et al., 1999; Gómez, 2004; Orsi and Tanksley, 2009). For example, the seedlings of large-seeded plants are better able to withstand resource restrictions and abiotic stresses, whereas small-seeded plants are thought to have superior colonization abilities because they produce large numbers of seeds (Westoby et al., 2002; Moles et al., 2005). In agriculture, seed size is one of the most important components of seed yield. Crop plants (e.g., rice [*Oryza sativa*] and wheat [*Triticum aestivum*]) have undergone selection for larger seed size during domestication (Fan et al., 2006; Song et al., 2007; Gegas et al., 2010). However, the genetic and molecular mechanisms of seed size control are poorly understood.

In flowering plants, the seed comprises three major anatomical components, the embryo, the endosperm, and the seed coat, each with different genetic compositions. Seed development involves a double fertilization process in which one sperm nucleus fuses with the egg cell to give rise to the diploid embryo, while the other sperm nucleus fuses with the central cell to produce the triploid endosperm (Lopes and Larkins, 1993). By contrast, the seed coat that surrounds the embryo and endosperm is typically of maternal origin. Therefore, the size of a seed is regulated by the coordinated growth of maternal sporophytic and zygotic tissues. Several factors that influence seed size by the zygotic tissues have been recently identified in *Arabidopsis thaliana*, including HAIKU1 (IKU1), IKU2, MINISEED3 (MINI3), and SHORT HYPOCOTYL UNDER BLUE1 (SHB1) (Garcia et al., 2003; Luo et al., 2005; Zhou et al., 2009; Wang et al., 2010). IKU1, IKU2, and MINI3 function in the same pathway of seed development (Garcia et al., 2003; Luo et al., 2005; Wang et al., 2010). Downregulation of these three genes results in precocious cellularization of the endosperm and subsequently decreased seed size at maturity (Garcia et al., 2003; Luo et al., 2005; Wang et al., 2010). SHB1 promotes endosperm growth in the early phase of seed development by binding *MINI3* and *IKU2* promoters (Zhou et al., 2009). Seed size is also strongly affected by maternal tissues. Several factors that act in maternal sporophytic tissues to regulate seed size have been described in *Arabidopsis*, such as TRANSPARENT TESTA GLABRA2 (TTG2), APETALA2 (AP2), AUXIN RESPONSE FACTOR2 (ARF2)/MEGAINTEGUMENTA (MNT), KLUH/CYTOCHROME P450 78A5 (KLU/CYP78A5), and ENHANCER3 OF DA1 (EOD3)/CYP78A6 (Garcia et al., 2005; Jofuku et al., 2005; Ohto et al., 2005, 2009; Schruff et al., 2006; Adamski et al., 2009; Fang et al., 2012). TTG2 and EOD3/CYP78A6 affect seed growth by increasing cell expansion in the integuments (Garcia et al., 2005; Ohto et al., 2009; Fang

[1] These authors contributed equally to this work.
[2] Address correspondence to yhli@genetics.ac.cn.
The author responsible for distribution of materials integral to the findings presented in this article in accordance with the policy described in the Instructions for Authors (www.plantcell.org) is: Yunhai Li (yhli@genetics.ac.cn).
[C] Some figures in this article are displayed in color online but in black and white in the print edition.
[W] Online version contains Web-only data.
www.plantcell.org/cgi/doi/10.1105/tpc.113.115063

et al., 2012), while AP2 may influence seed growth by limiting cell expansion in the integuments (Jofuku et al., 2005; Ohto et al., 2005, 2009). By contrast, KLU/CYP78A5 promotes seed growth by increasing cell proliferation in the integuments of ovules (Adamski et al., 2009), whereas ARF2/MNT restricts seed size by decreasing cell proliferation in the integuments (Schruff et al., 2006; Li et al., 2008). Therefore, the proliferation of integument cells to form the seed coat plays a critical role in setting seed size.

Several factors involved in ubiquitin-related activities have been known to influence seed size. A growth-restricting factor, DA1, is a ubiquitin receptor containing two ubiquitin interaction motifs (UIMs) that bind ubiquitin in vitro, and the *da1-1* mutant forms large seeds as a result of changes in the maternal integuments of ovules (Li et al., 2008). Mutations in an enhancer of *da1-1* (*EOD1*), which encodes the E3 ubiquitin ligase BIG BROTHER (BB; Disch et al., 2006; Li et al., 2008), synergistically enhance the seed size phenotype of *da1-1*, indicating that *DA1* acts synergistically with *EOD1*/*BB* to regulate seed size. In rice, a quantitative trait locus for *GRAIN WIDTH AND WEIGHT2* (*GW2*), encoding an E3 ubiquitin ligase, regulates grain size by restricting cell division (Song et al., 2007). An uncharacterized protein encoded by rice *QTL FOR SEED WIDTH ON CHROMOSOME5*/*GW5* is required to limit grain size in rice (Shomura et al., 2008; Weng et al., 2008). GW5 physically interacts with polyubiquitin in a yeast two-hybrid assay, suggesting that GW5 may be involved in the ubiquitin-proteasome pathway (Weng et al., 2008). However, it is not clear whether these two factors act in maternal and/or zygotic tissues in rice.

To understand the molecular mechanisms of seed size control, we previously identified *da* mutants with large seeds in *Arabidopsis* (Li et al., 2008). Here, we describe *Arabidopsis DA2*, encoding a Really Interesting New Gene (RING)-type protein with E3 ubiquitin ligase activity, which acts maternally to restrict seed growth. Genetic analyses show that DA2 functions synergistically with the ubiquitin receptor DA1 to regulate seed size, but does so independently of the E3 ubiquitin ligase EOD1. We further demonstrate that DA1 interacts physically with DA2 in vitro and in vivo. Overexpression of rice *GW2*, a homolog of *DA2*, restricts seed and organ growth in *Arabidopsis*, suggesting a possible conserved function in *Arabidopsis* and rice. Thus, our findings define the genetic and molecular mechanisms of three ubiquitin-related proteins, DA1, DA2, and EOD1, in seed size regulation and suggest that combining the effects of DA1, DA2, and EOD1 from different seed crops provides a promising strategy for engineering crops with large seeds.

RESULTS

The *da2-1* Mutant Produces Large Seeds

We previously identified a ubiquitin receptor, DA1, and an E3 ubiquitin ligase, EOD1/BB, as important factors influencing seed size in *Arabidopsis* (Li et al., 2008), suggesting that the ubiquitin pathway plays an important part in seed growth. To further understand the mechanisms of ubiquitin-mediated regulation of seed size, we collected the publicly available T-DNA insertion lines of some predicted ubiquitin ligase genes that were expressed in *Arabidopsis* ovules and/or seeds in several microarray studies (http://affymetrix.Arabidopsis.info/narrays/digitalnorthern.pl) and investigated their seed growth phenotypes. From this screen, we identified several T-DNA insertion mutants with altered seed size. We designated one of these mutants *da2-1*, referring to the order of discovery for large seed size mutants (DA means "large" in Chinese). Seeds produced by *da2-1* were larger and heavier than the wild-type seeds (Figures 1A, 2A, 2C, and 2D). Seed number per silique and seed yield per plant in *da2-1* were slightly higher than those in the wild type (Figures 1B and 1C). By contrast, the total number of seeds per plant in *da2-1* was not significantly increased, compared with that in the wild type (Figure 1D). The *da2-1* plants were higher than wild-type plants at the mature stage (Figure 1E). In addition, *da2-1* mutant plants formed large flowers and leaves as well as increased biomass compared with wild-type plants (Figures 1F and 1G; see Supplemental Figures 1A to 1C online). The increased size of *da2-1* mutant petals and leaves was not caused by larger cells (see Supplemental Figures 1D and 1E online), indicating that it is the number of petal and leaf cells that is higher.

DA2 Acts Synergistically with *DA1* to Regulate Seed Size, but Does So Independently of *EOD1*

The seeds of the *da2-1* mutant were enlarged, but not to the same extent as in *da1-1* (Li et al., 2008), suggesting that *DA1* and *DA2* could function in a common pathway. To test for a genetic interaction between *DA1* and *DA2*, we generated a *da1-1 da2-1* double mutant and determined its seed size. Although the *da2-1* mutant had slightly larger and heavier seeds than the wild type (Figures 1A, 2C, and 2D; see Supplemental Figure 2B online), the *da2-1* mutation synergistically enhanced the seed size and weight phenotypes of *da1-1* (Figures 2A and 2C; see Supplemental Figure 2B online), revealing a synergistic genetic interaction between *DA1* and *DA2* in seed size. The changes in seed size were reflected in the size of the embryos and resulting seedlings (Figure 2B; see Supplemental Figure 2A online). We further measured the cotyledon area of 10-d-old seedlings. A synergistic enhancement of cotyledon size of *da1-1* by the *da2-1* mutation was also observed (Figures 2B and 2E).

The mutant protein encoded by the *da1-1* allele has negative activity toward DA1 and a DA1-related protein (DAR1), its closest homolog (Li et al., 2008). Double *da1-knockout1* (*da1-ko1*) *dar1-1* T-DNA insertion mutants exhibited the *da1-1* phenotypes, while *da1-ko1* and *dar1-1* single mutants did not show an obvious seed size phenotype (Li et al., 2008). As *da1-1* and *da2-1* act synergistically to increase seed size, one would expect that *da1-ko1* might synergistically enhance the phenotypes of *da2-1*. To test this, we generated the *da1-ko1 da2-1* double mutant. As shown in Figure 2D and Supplemental Figure 2C online, the seed size and weight phenotypes of *da2-1* were also synergistically enhanced by the *da1-ko1* mutation. We further measured cotyledon area of 10-d-old seedlings. The *da1-ko1* mutation synergistically enhanced the cotyledon size phenotype of *da2-1* (Figure 2F). Similarly, a synergistic enhancement of petal size of *da2-1* by the *da1-ko1* mutation was also observed (see Supplemental Figure 2D online). These results further demonstrate the synergistic effects

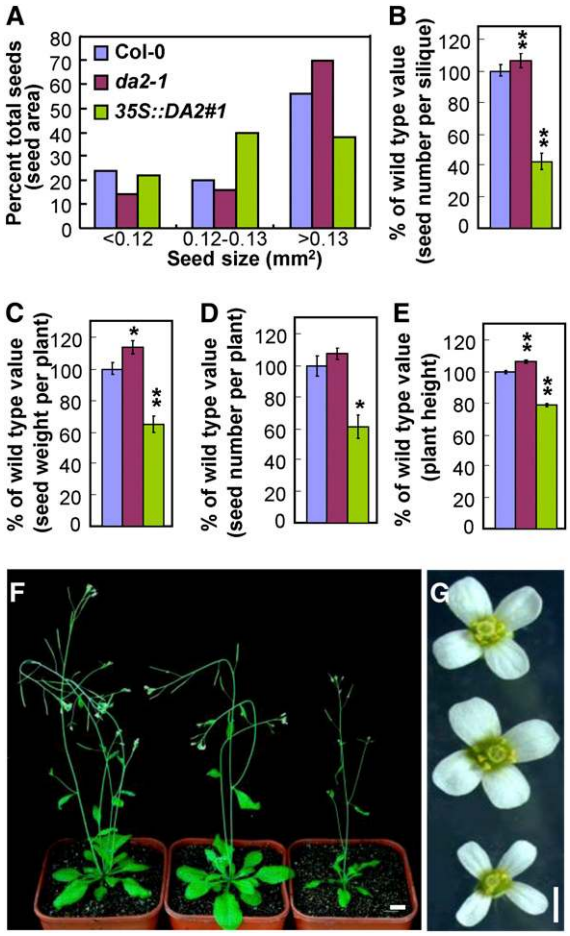

Figure 1. Seed and Organ Size in the *da2-1* Mutant.

(A) Projective area of Col-0, *da2-1*, and *35S:DA2#1* seeds. The seeds were classified into three groups (>0.13, 0.12 to 0.13, and < 0.12 mm^2). Values for each group are expressed as a percentage of the total seed number analyzed.

(B) Seed number per silique for Col-0, *da2-1*, and *35S:DA2#1*. Siliques (from the fourth silique to the tenth silique) on the main stem were used to measure seed number per silique (n = 20).

(C) Seed weight per plant for Col-0, *da2-1*, and *35S:DA2#1*. Seed weight was determined from 15 independent plants for each genotype (n = 15).

(D) Seed number per plant for Col-0, *da2-1*, and *35S:DA2#1*. Seed weight was determined from 15 independent plants for each genotype (n = 15).

(E) Height of Col-0, *da2-1*, and *35S:DA2#1* plants. Plant height was determined from 20 independent plants for each genotype (n = 20).

(F) Thirty-four-day-old plants of Col-0 (left), *da2-1* (middle), and *35S:DA2#1* (right).

(G) Flowers of Col-0 (top), *da2-1* (middle), and *35S:DA2#1* (bottom).

Values in **(B)** to **(E)** are given as mean ± SE relative to the wild-type value, set at 100%. **P < 0.01 and *P < 0.05 compared with the wild type (Student's t test).

Bars = 1 cm in **(F)** and 1 mm **(G)**.

[See online article for color version of this figure.]

of the simultaneous disruption of both *DA1* and *DA2*. We further measured the size of embryo cells and petal epidermal cells. Cell size in *da1-1 da2-1* and *da1-ko1 da2-1* double mutants was not increased, compared with that measured in their parental lines (Figure 2G; see Supplemental Figure 2E online), suggesting that *DA1* and *DA2* act synergistically to restrict cell proliferation.

The *da1-1 da2-1* double mutant had larger seeds than *da1-ko1 da2-1* (Figures 2C, 2D, and 2H; see Supplemental Figures 2B and 2C online), which is consistent with our previous report that the *da1-1* allele had stronger phenotypes than *da1-ko1* (Li et al., 2008). The size of *da1-1* seeds was similar to that of *da1-ko1 dar1-1* double mutant seeds because the *da1-1* allele has a negative effect on DA1 and DAR1 (Figure 2H) (Li et al., 2008). Therefore, one would expect that the size of *da1-1 da2-1* double mutant seeds might be similar to that of *da1-ko1 dar1-1 da2-1* triple mutant seeds. We therefore generated a *da1-ko1 dar1-1 da2-1* triple mutant and investigated its seed size. As shown in Figure 2H, the size of *da1-ko1 dar1-1 da2-1* triple mutant seeds was comparable with that of *da1-1 da2-1* double mutant seeds, but larger than that of *da1-ko1 da2-1* double mutant seeds. Thus, these genetic analyses further support that the *da1-1* allele has a negative effect on both DA1 and DAR1 (Li et al., 2008).

We previously identified an enhancer of *da1-1* (*EOD1*), which is allelic to *BB* (Disch et al., 2006; Li et al., 2008). The *eod1* mutations synergistically enhanced the seed size phenotype of *da1-1* (Li et al., 2008). Similarly, the seed size and weight phenotypes of *da2-1* were synergistically enhanced by *da1-1* and *da1-ko1* (Figures 2A, 2C, and 2D). We therefore asked whether *DA2* and *EOD1* could function in a common pathway. To determine the genetic relationship between *DA2* and *EOD1*, we analyzed an *eod1-2 da2-1* double mutant. The genetic interaction between *eod1-2* and *da2-1* was essentially additive for both seed weight and petal size compared with their parental lines (see Supplemental Figures 2F and 2G online), suggesting that *DA2* functions to influence seed and organ growth separately from *EOD1*.

DA2 Acts Maternally to Influence Seed Size

Considering that the size of seeds is affected by the maternal and/or zygotic tissues, we asked whether *DA2* functions maternally or zygotically. To test this, we performed reciprocal cross experiments between the wild type and *da2-1*. As shown in Figure 3E, the effect of *da2-1* on seed size was observed only when maternal plants are homozygous for the *da2-1* mutation. Seeds produced by maternal *da2-1* plants, regardless of the genotype of the pollen donor, were consistently larger than those produced by maternal wild-type plants. This result indicates that *da2-1* can act maternally to influence seed size. We previously demonstrated that *DA1* also functions maternally to regulate seed size (Li et al., 2008). As the *da1-ko1* mutation synergistically enhanced the seed size phenotype of *da2-1* (Figure 2D), we further conducted reciprocal cross experiments between the wild type and *da1-ko1 da2-1* double mutant. Similarly, the effect of *da1-ko1 da2-1* on seed size was observed only when *da1-ko1 da2-1* acted as the maternal plant (Figure 3F). Pollinating *da1-ko1*/+ *da2-1*/+ plants with *da1-ko1 da2-1* double mutant pollen leads to the development of *da1-ko1 da2-1*, *da1-ko1*/*da1-ko1 da2-1*/+, *da1-ko1*/+ *da2-1 da2-1*, and *da1-ko1*/+ *da2-1*/+ embryos within *da1-ko1*/+

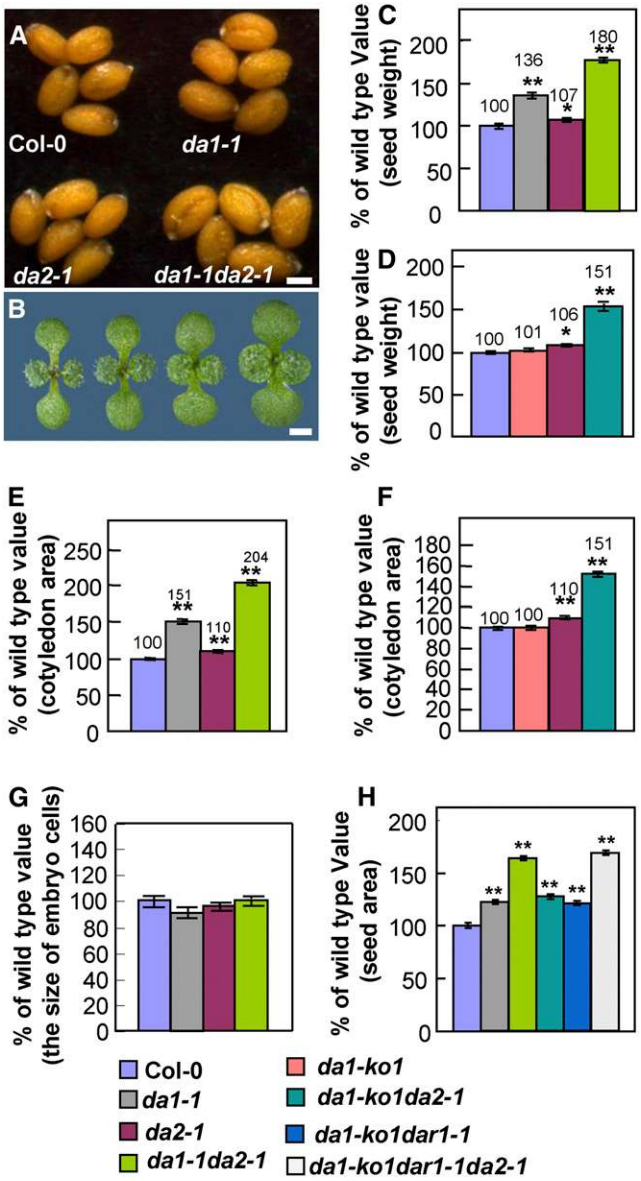

Figure 2. *DA1* and *DA2* Act Synergistically to Control Seed Size.

(A) Dry seeds of Col-0, *da1-1*, *da2-1*, and *da1-1 da2-1*.

(B) Ten-day-old seedlings of Col-0, *da2-1*, *da1-1*, and *da1-1 da2-1* (from left to right).

(C) Seed weight of Col-0, *da1-1*, *da2-1*, and *da1-1 da2-1*. Seed weight was determined by weighing mature dry seeds in batches of 500. The weights of five sample batches were measured for each seed lot ($n = 5$).

(D) Seed weight of Col-0, *da1-ko1*, *da2-1*, and *da1-ko1 da2-1*. Seed weight was determined by weighing mature dry seeds in batches of 500. The weights of five sample batches were measured for each seed lot ($n = 5$).

(E) Cotyledon area of 10-d-old Col-0, *da1-1*, *da2-1*, and *da1-1 da2-1* seedlings ($n = 35$).

(F) Cotyledon area of 10-d-old Col-0, *da1-ko1*, *da2-1*, and *da1-ko1 da2-1* seedlings ($n = 35$).

(G) The average area of palisade cells in cotyledons of Col-0, *da1-1*, *da2-1*, and *da1-1 da2-1* embryos ($n = 120$).

da2-1/+ seed coats. We further measured the size of individual seeds from *da1-ko1*/+ *da2-1*/+ plants fertilized with *da1-ko1 da2-1* double mutant pollen and genotyped *da1-ko1* and *da2-1* mutations. Our results show that *da1-ko1* and *da2-1* mutations are not associated with variation in the size of these seeds (Figure 3G). Together, these analyses indicate that the embryo and endosperm genotypes for *DA1* and *DA2* do not affect seed size, and *DA1* and *DA2* are required in sporophytic tissue of the mother plant to regulate seed growth.

DA2 Acts Synergistically with *DA1* to Affect Cell Proliferation in the Maternal Integuments

Reciprocal crosses showed that *DA1* and *DA2* function maternally to determine seed size (Figures 3E to 3G) (Li et al., 2008). The integuments surrounding the ovule are maternal tissues and form the seed coat, which may physically restrict seed growth, after fertilization. Several studies showed that the integument size of ovules determines seed size (Schruff et al., 2006; Adamski et al., 2009). We therefore asked whether *DA1* and *DA2* act through the maternal integuments to regulate seed size. To test this, we investigated mature ovules from the wild type, *da1-1*, *da2-1*, and *da1-1 da2-1* at 2 d after emasculation. The size of *da1-1* ovules was dramatically larger than that of wild-type ovules (Figures 3A, 3B, and 3H), consistent with our previous findings (Li et al., 2008). The *da2-1* ovules were also larger than wild-type ovules (Figures 3A, 3C, and 3H). The *da2-1* mutation synergistically enhanced the ovule size phenotype of *da1-1* (Figures 3A to 3D and 3H), consistent with their synergistic interactions in seed size.

The size of the integument or seed coat is determined by cell proliferation and cell expansion. After fertilization, cells in integuments mainly undergo expansion, but still carry on proliferation (Garcia et al., 2005). A previous study showed that the integument of a developing seed ceases cell division at 4 d after pollination (DAP) (Garcia et al., 2005). We therefore investigated the outer integument cell number of developing seeds in the wild type, *da1-1*, *da2-1*, and *da1-1 da2-1* at 6 and 8 DAP. In wild-type seeds, the number of outer integument cells at 6 DAP was similar to that at 8 DAP (Figure 3I), indicating that cells in the outer integuments of wild-type seeds completely stop division at 6 DAP. Similarly, cells in the outer integuments of *da1-1*, *da2-1*, and *da1-1 da2-1* seeds completely stopped cell proliferation at 6 DAP (Figure 3I). The number of outer integument cells in *da1-1* and *da2-1* seeds was significantly increased compared with that in wild-type seeds (Figure 3I). The *da2-1* mutation synergistically enhanced the outer integument cell number of *da1-1* (Figure 3I). We further investigated the outer integument cell length of wild-type, *da1-1*, *da2-1*, and *da1-1 da2-1* seeds at 6 and 8 DAP. Cells in *da1-1*, *da2-1*, and *da1-1 da2-1* outer integuments were significantly shorter than

(H) Projective area of Col-0, *da1-1*, *da1-1 da2-1*, *da1-ko1 da2-1*, *da1-ko1 dar1-1*, and *da1-ko1 dar1-1 da2-1* seeds ($n = 120$).

Values in **(C)** to **(H)** are given as mean ± SE relative to the respective wild-type values, set at 100%. **P < 0.01 and *P < 0.05 compared with the wild type (Student's *t* test).

Bars = 0.1 mm in **(A)** and 1 mm in **(B)**.

[See online article for color version of this figure.]

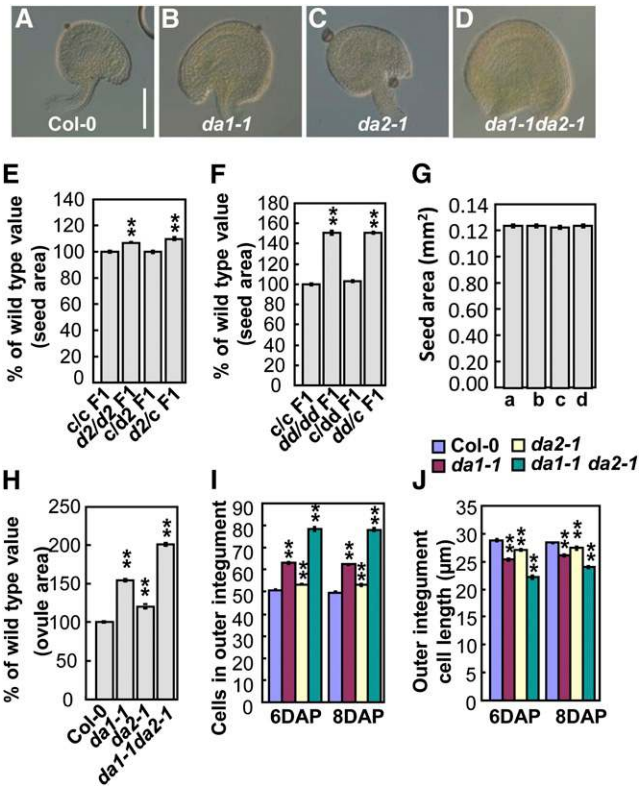

Figure 3. *DA1* and *DA2* Act Synergistically to Regulate Cell Proliferation in Maternal Integuments of Developing Seeds.

(A) to **(D)** Mature ovules of Col-0, *da1-1*, *da2-1*, and *da1-1 da2-1*. The *da2-1* mutation synergistically enhances the ovule size of *da1-1*.

(E) Projective area of Col-0 × Col-0 (c/c) F1, *da2-1* × *da2-1* (d2/d2) F1, Col-0 × *da2-1* (c/d2) F1, and *da2-1* × Col-0 (d2/c) F1 seeds (n = 120).

(F) Projective area of Col-0 × Col-0 (c/c) F1, *da1-ko1 da2-1* × *da1-ko1 da2-1* (dd/dd) F1, Col-0 × *da1-ko1 da2-1* (c/dd) F1, *da1-ko1 da2-1* × Col-0 (dd/c) F1 seeds (n = 120).

(G) Pollinating *da1-ko1*/+ *da2-1*/+ plants with *da1-ko1 da2-1* double mutant pollen leads to the development of *da1-ko1*/+ *da2-1*/+ (a), *da1-ko1*/+ *da2-1da2-1* (b), *da1-ko1*/*da1-ko1 da2-1*/+ (c), and *da1-ko1 da2-1* (d) embryos within *da1-ko1*/+ *da2-1*/+ seed coats. Projective area of individual seeds from *da1-ko1*/+*da2-1*/+ plants fertilized with *da1-ko1 da2-1* double mutant pollen was measured (n = 50). These seeds were further genotyped for *da1-ko1* and *da2-1* mutations. The data show that *da1-ko1* and *da2-1* mutations are not associated with variation in the size of these seeds ($P > 0.05$, Student's t test).

(H) Projective area of Col-0, *da1-1*, *da2-1*, and *da1-1 da2-1* mature ovules (n = 120).

(I) The number of cells in the outer integuments of Col-0, *da1-1*, *da2-1*, and *da1-1 da2-1* seeds at 6 and 8 DAP. Thirty seeds for each genotype were examined (n = 30).

(J) Average length of cells in the outer integuments of Col-0, *da1-1*, *da2-1*, and *da1-1 da2-1* seeds at 6 and 8 DAP calculated from the outer integument length and cell number for individual seeds. Thirty seeds for each genotype were examined (n = 30).

Values in **(E)**, **(F)**, and **(H)** are given as mean ± SE relative to the respective wild-type values, set at 100%. **$P < 0.01$ compared with the wild type (Student's t test).

Bars = 0.5 mm in **(A)** to **(D)**.

[See online article for color version of this figure.]

those in wild-type outer integuments (Figure 3J), suggesting a possible compensation mechanism between cell proliferation and cell expansion in the integuments. Thus, these results show that *DA2* acts synergistically with *DA1* to restrict cell proliferation in the maternal integuments.

DA2 Encodes a Functional E3 Ubiquitin Ligase

The *da2-1* mutation was identified as having a T-DNA insertion in the seventh exon of the gene At1g78420 (Figure 4A). The T-DNA insertion site was further confirmed by PCR using T-DNA–specific and flanking primers and sequencing the PCR products (see Supplemental Figures 3A and 3B online). The full-length mRNA of At1g78420 could not be detected in *da2-1* mutant (see Supplemental Figure 3C online). We expressed At1g78420 coding DNA sequence under the control of its own promoter in *da2-1* plants and isolated 62 transgenic plants. Nearly all transgenic lines exhibited complementation of *da2-1* phenotypes (Figures 4D to 4F), indicating that At1g78420 is *DA2*.

To further characterize *DA2* function, in particular gain-of-function phenotypes, we expressed the coding region of *DA2* under the control of the cauliflower mosaic virus 35S promoter in wild-type plants and isolated 77 transgenic plants. Overexpression of *DA2* caused decreases in seed size, seed yield per plant, and seed number per plant (Figures 1A, 1C, and 1D). In addition, most transgenic plants overexpressing *DA2* had small flowers and leaves, short siliques, reduced plant height, as well as decreased biomass compared with the wild type (Figures 1E to 1G; see Supplemental Figures 1A to 1C and Supplemental Figure 4 online). These results further support the role of *DA2* in limiting seed and organ growth.

DA2 is predicted to encode a 402–amino acid protein containing one predicted RING domain (59-101) (Figure 4B; see Supplemental Figure 5 online). Previous research showed that RING-type proteins can act as E3 ubiquitin ligases that function as adapters that transfer ubiquitin from E2 ubiquitin ligases to target proteins (Seo et al., 2003). To investigate whether DA2 has E3 ubiquitin ligase activity, we expressed DA2 in *Escherichia coli* as a fusion protein with maltose binding protein (MBP) and purified MBP-DA2 protein from the soluble fraction. In the presence of an E1 ubiquitin activating enzyme, an E2-conjugating enzyme, His-ubiquitin, and MBP-DA2, a polyubiquitination signal, were observed by immunoblot using an anti-His antibody (Figure 4C, fifth lane from the left). The anti-MBP blot analysis also showed that MBP-DA2 was ubiquitinated (Figure 4C, fifth lane from the left). However, in the absence of E1, E2, His-ubiquitin, or MBP-DA2, no polyubiquitination was detected (Figure 4C, first to fourth lanes from the left), demonstrating that DA2 is a functional E3 ubiquitin ligase.

The RING motif is essential for the E3 ubiquitin ligase activity of RING finger proteins (Xie et al., 2002). Therefore, we tested whether an intact RING finger domain was required for DA2 E3 ligase activity. A single amino acid substitution allele was produced by mutagenizing Cys-59 to Ser (C59S), as this mutation is predicted to disrupt the RING domain (see Supplemental Figure 5 and Supplemental Data Set 1 online). An in vitro ubiquitination assay indicated that the E3 ligase activity was abolished in the C59S mutant of DA2 (Figure 4C, sixth lane from the left), indicating

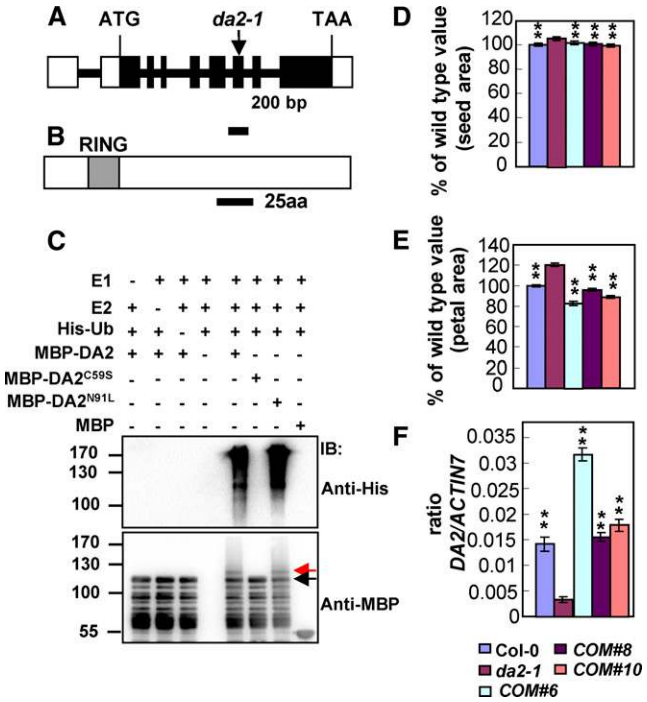

Figure 4. Identification and Molecular Characterization of *DA2.*

(A) The *DA2* gene structure. The start codon (ATG) and the stop codon (TAA) are indicated. Closed boxes indicate the coding sequence, open boxes indicate the 5′ and 3′ untranslated regions, and lines between boxes indicate introns. The T-DNA insertion site (*da2-1*) in *DA2* is shown.
(B) DA2 contains a predicted RING domain. aa, amino acids.
(C) E3 ubiquitin ligase activity of DA2. MBP-DA2 and mutated DA2 (MBP-DA2^{C59S} and MBP-DA2^{N91L}) fusion proteins were assayed for E3 ubiquitin ligase activity in the presence of E1, E2, and His-ubiquitin (His-Ub). Ubiquitinated proteins were detected by immunoblotting (IB) with anti-His antibody and anti-MBP antibody, respectively. The black arrow indicates MBP-DA2 proteins, and the red arrow shows ubiquitinated MBP-DA2 proteins.
(D) Projective area of Col-0, *da2-1*, *COM#6, COM#8*, and *COM#10* seeds (n = 120). *COM* is *da2-1* transformed with the *DA2* coding sequence driven by its own promoter.
(E) Petal area of Col-0, *da2-1*, *COM#6*, *COM#8*, and *COM#10* plants (n = 50).
(F) Quantitative real-time RT-PCR analysis of *DA2* expression in Col-0, *da2-1*, *COM#6*, *COM#8*, and *COM#10* seedlings. Three biological replicates, each consisting of three technical replicates, were performed (n = 3). Values in **(D)** to **(F)** are given as mean ± SE relative to the *da2-1* values, set at 100%. **P < 0.01 compared with the *da2-1* mutant (Student's *t* test).
[See online article for color version of this figure.]

that an intact RING domain is required for DA2 E3 ubiquitin ligase activity. We further overexpressed *DA2^{C59S}* (*35S:DA2^{C59S}*) in wild-type Columbia-0 (Col-0) plants and isolated 69 transgenic plants. The seed and petal size of transgenic plants was comparable with that of wild-type plants, although transgenic plants had high expression levels of *DA2^{C59S}* (see Supplemental Figures 6A to 6C online), indicating that the *DA2^{C59S}* mutation affects the function of *DA2* in seed and organ growth.

Three RING types, RING-H2, RING-HCa, and RING-HCb, and five modified RING types, RING-C2, RING-v, RING-D, RING-S/T, and RING-G, have been described in *Arabidopsis* (Stone et al., 2005). A new type of RING domain (C5HC2) found in rice GW2 has been proposed (Song et al., 2007). Although the spacing of the Cys residues in the predicted RING domain of DA2 was similar to that in the RING domain (C5HC2) of rice GW2, the RING domain of DA2 lacked a conserved His residue that was replaced by an Asn residue (Asn-91) (see Supplemental Figure 5 and Supplemental Data Set 1 online). This amino acid substitution was also observed in the predicted RING domain of DA2 homologs in dicots, such as soybean (*Glycine max*) and oilseed rape (*Brassica napus*) (see Supplemental Figure 5 and Supplemental Data Set 1 online). We therefore asked whether this Asn residue (Asn-91) is crucial for its E3 ubiquitin ligase activity. A single amino acid substitution allele was produced by mutagenizing Asn-91 to Leu (N91L). An in vitro ubiquitination assay showed that the N91L mutant of DA2 had the E3 ligase activity (Figure 4C, the seventh lane from the left), suggesting that Asn-91 may not be required for DA2 E3 ligase activity. These results suggest that the RING domain of DA2 might be a variant of that found in GW2. We further overexpressed *DA2^{N91L}* (*35S:DA2^{N91L}*) in wild-type plants and isolated 26 transgenic plants. The seeds of transgenic plants were smaller than wild-type seeds (see Supplemental Figures 6D and 6E online), suggesting that the *DA2^{N91L}* could restrict seed growth.

Homologs of *Arabidopsis* DA2

Proteins that share significant homology with DA2 outside of the RING domain are found in *Arabidopsis* and crop plants, including oilseed rape, soybean, rice, maize (*Zea mays*), and barley (*Hordeum vulgare*) (see Supplemental Data Set 1 and Supplemental Figure 7 online). One predicted protein in *Arabidopsis* shares extensive amino acid similarity with DA2 and is named DA2-like protein (DA2L; At1g17145) (see Supplemental Data Set 1 and Supplemental Figure 7 online). Like *35S:DA2* plants, *DA2L*-overexpressing lines exhibited small plants and organs (see Supplemental Figure 8 online), suggesting that *DA2* and *DA2L* have similar functions. The similar proteins in other plant species show a 39.2 to 84.5% amino acid sequence identity with DA2 (see Supplemental Data Set 1 and Supplemental Figure 7 online). The homolog in oilseed rape had the highest amino acid sequence identity with DA2 (84.5%) (see Supplemental Data Set 1 and Supplemental Figure 7 online). Rice GW2 had 43.1% amino acid sequence identity with *Arabidopsis* DA2 (see Supplemental Data Set 1 and Supplemental Figure 7 online). As overexpression of *GW2* reduced grain width in rice (Song et al., 2007), we asked whether *DA2* and *GW2* perform similar functions in seed size regulation. We therefore overexpressed *GW2* in wild-type plants. Like *35S:DA2* and *35S:DA2L* transgenic lines, the *Arabidopsis* transgenic plants overexpressing *GW2* produced smaller seeds and organs than wild-type plants (see Supplemental Figure 9 online), suggesting a possible conserved function for *Arabidopsis DA2* and rice *GW2* in seed and organ growth regulation.

DA2 and *DA1* Show Similar Expression Patterns

To determine the expression pattern of *DA2*, RNA from roots, stems, leaves, seedlings, and inflorescences was analyzed by

quantitative real-time RT-PCR analysis. *DA2* mRNA was detected in all plant organs tested (Figure 5A). The tissue-specific expression patterns of *DA2* were investigated using histochemical assay of β-glucuronidase (GUS) activity of transgenic plants containing a *DA2* promoter:*GUS* fusion (*pDA2*:*GUS*). GUS activity was detected in roots, cotyledons, leaves, and inflorescences (Figures 5B and 5C). Relatively high GUS activity was detected in leaf primordia and roots (Figures 5B and 5C). In flowers, relatively stronger expression of *DA2* was observed in young floral organs than old floral organs (Figures 5D to 5L). Similarly, higher GUS activity was detected in younger ovules than older ones (Figures 5M and 5N). This shows that *DA2* expression is regulated temporally and spatially. We previously reported that *DA1* was highly expressed during early stages of organ formation, but levels were largely reduced at the later stages of organ development (Li et al., 2008). Together, these results suggest that *DA1* and *DA2* have similar expression patterns during organ development.

DA1 Interacts with DA2 in Vitro and in Vivo

Our genetic analyses show that DA1 acts synergistically with DA2 to restrict seed and organ growth. Such synergies can be caused by simultaneously disrupting two components of a protein complex (Pérez-Pérez et al., 2009; Lanctot et al., 2013). In addition, ubiquitin receptors have been reported to interact with E3 ubiquitin ligases and influence the degradation of their ubiquitinated substrates in animals (Alexandru et al., 2008; Bandau et al., 2012). We therefore assessed whether DA1 interacts with the E3 ubiquitin ligase DA2 using an in vitro interaction/pull-down experiment. DA1 was expressed as a glutathione *S*-transferase (GST) fusion protein, while DA2 was expressed as a MBP fusion protein. As shown in Figure 6A (first and second lanes from left), GST-DA1 bound to MBP-DA2, while GST-DA1 did not bind to a negative control (MBP). This result indicates that DA1 physically interacts with DA2 in vitro.

DA1 contains two UIMs, a single LIM domain defined by its conservation with the canonical Lin-11, Isl-1, and Mec3 domains and the highly conserved C-terminal region (Figure 6B) (Li et al., 2008). We further asked which domain of DA1 is required for the interaction between DA1 and DA2. A series of DA1 derivatives containing specific protein domains were expressed in *E. coli*: DA1-UIM, containing only the two UIM domains; DA1-LIM, with only the LIM domain; DA1-LIM+C, containing only the LIM domain and the C-terminal region; and DA1-C, with only the C-terminal region, were expressed as GST fusion proteins (Figure 6B). DA2 was expressed as an MBP fusion protein and used in pull-down experiments. As shown in Figure 6A, GST-DA1-LIM+C and GST-DA1-C interacted with MBP-DA2, but GST-DA1-UIM and GST-DA1-LIM did not bind to MBP-DA2. This result indicates that the conserved C-terminal region of DA1 interacts with DA2.

Considering that the mutant protein encoded by the *da1-1* allele ($DA1^{R358K}$) has a mutation in the C-terminal region (Figure 6B) (Li et al., 2008), we asked whether the $DA1^{R358K}$ mutation affects interactions with DA2. Using a GST-$DA1^{R358K}$ fusion protein in pull-down experiments with MBP-DA2, we showed that the mutation in $DA1^{R358K}$ does not affect the interaction between DA1 and DA2 (Figure 6A, third lane from left).

To further investigate the possible association between DA1 and DA2 in planta, we used coimmunoprecipitation analysis to detect their interactions in vivo. We transiently coexpressed *35S*:*Myc-DA1* and *35S*:*GFP-DA2* in *Nicotiana benthamiana* leaves. Transient coexpression of *35S*:*GFP* and *35S*:*Myc-DA1* in *N. benthamiana* leaves was used as a negative control. Total proteins were isolated and incubated with GFP-Trap-A agarose beads to immunoprecipitate GFP-DA2 or GFP. Precipitates were detected with anti-GFP and anti-Myc antibodies, respectively. As shown in Figure 6C, Myc-DA1 was detected in the immunoprecipitated GFP-DA2 complex but not in the negative control (GFP), indicating that there is a physical association between DA1 and DA2 in planta. As the C-terminal region of DA1 interacted with DA2 in the pull-down assay (Figure 6A), we further asked whether the C terminus of DA1 interacts with DA2 in planta. The coimmunoprecipitation analysis showed that the C-terminal region of DA1 (Myc-DA1-C) was detected in the GFP-DA2 complex but not in the negative control (PEX10-GFP, a RING-type E3 ubiquitin ligase) (see Supplemental Figure 10 online) (Platta et al., 2009; Kaur et al., 2013). Thus, these results indicate that the C-terminal region of DA1 is required for the interaction with DA2 in vitro and in vivo.

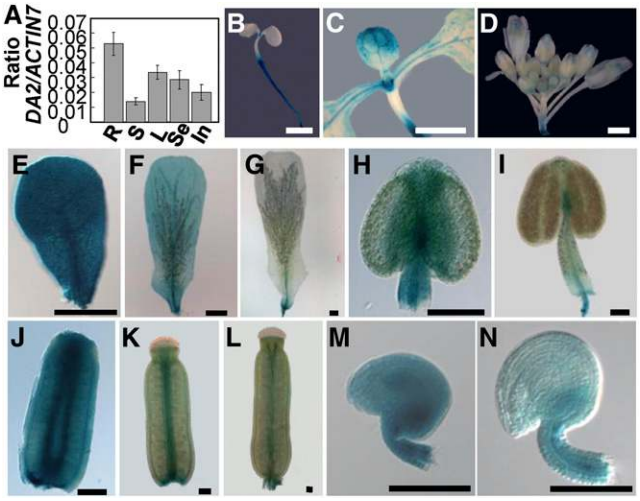

Figure 5. Expression Patterns of *DA2*.

(A) Quantitative real-time RT-PCR analysis of *DA2* expression. Total RNA was isolated from roots (R), stems (S), leaves (L), seedlings (Se), and inflorescences (In).

(B) to **(N)** *DA2* expression activity was monitored by *pDA2*:*GUS* transgene expression. Four GUS-expressing lines were observed, and all showed a similar pattern, although they differed slightly in the intensity of the staining. Histochemical analysis of GUS activity in a 4-d-old seedling **(B)**, a 10-d-old seedling **(C)**, a floral inflorescence **(D)**, the developing petals **([E]** to **[G])**, the developing stamens **([H]** and **[I])**, the developing carpels **([J]** to **[L])**, and the developing ovules **([M]** and **[N])**. Bars =1 mm in **(B)** to **(D)** and 0.1 mm in **(E)** to **(N)**.

[See online article for color version of this figure.]

DISCUSSION

Seed size in higher plants is a key determinant of evolutionary fitness and is an important agronomic trait in crop domestication

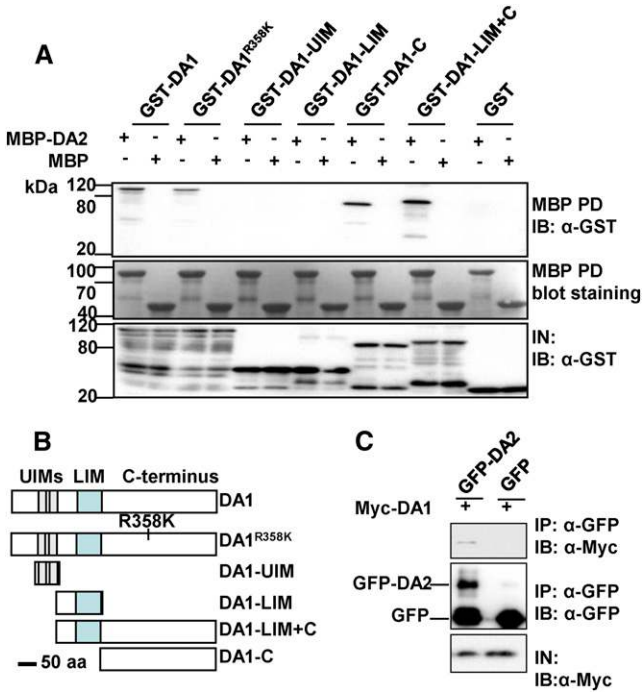

Figure 6. DA1 Interacts with DA2 in Vitro and in Vivo.

(A) DA1 directly interacts with DA2 in vitro. GST-DA1, GST-DA1^{R358K}, GST-DA1-UIM, GST-DA1-LIM, GST-DA1-LIM+C, and GST-DA1-C were pulled down (PD) by MBP-DA2 immobilized on amylose resin and analyzed by immunoblotting (IB) using an anti-GST antibody.

(B) Schematic diagram of DA1 and its derivatives containing specific protein domains. The predicted DA1 protein contains two UIM motifs, a single LIM domain, and the C-terminal region. aa, amino acids.

(C) DA1 interacts with DA2 in vivo. *N. benthamiana* leaves were transformed by injection of *Agrobacterium* GV3101 cells harboring *35S:Myc-DA1* and *35S:GFP-DA2* plasmids. Total proteins were immunoprecipitated with GFP-Trap-A, and the immunoblot was probed with anti-GFP and anti-Myc antibodies, respectively.

Myc-DA1 was detected in the immunoprecipitated GFP-DA2 complex, indicating that there is a physical association between DA1 and DA2 in planta.

[See online article for color version of this figure.]

(Gómez, 2004; Orsi and Tanksley, 2009). Several factors that act maternally to regulate seed size have been identified, such as ARF2/MNT, AP2, KLU/CYP78A5, EOD3/CYP78A6, and DA1. However, the genetic and molecular mechanisms of these factors in seed size regulate are nearly totally unknown. We previously demonstrated that the ubiquitin receptor DA1 acts synergistically with the E3 ubiquitin ligase EOD1/BB to regulate seed size (Li et al., 2008). In this study, we identified *Arabidopsis* DA2 as another RING E3 ubiquitin ligase involved in regulating seed size. Genetic analyses show that DA2 functions synergistically with DA1 to regulate final seed size, but does so independently of the E3 ubiquitin ligase EOD1. We further revealed that DA1 interacts physically with DA2. Our results define a ubiquitin-based system involving DA1, DA2, and EOD1 that controls final seed size in *Arabidopsis*.

DA2 Acts Maternally to Regulate Seed Size

The *da2-1* loss-of-function mutant formed large seeds and organs, whereas plants overexpressing *DA2* produced small seeds and organs (Figures 1A, 1F, and 1G), indicating that DA2 is a negative factor of seed and organ size regulation. Surprisingly, *Arabidopsis* DA2 was recently proposed to function as a positive regulator of organ growth, although nothing is known about how DA2 regulates seed and organ growth (Van Daele et al., 2012). In this study, we have sufficient evidence to prove that DA2 is a negative regulator of seed and organ growth. The *da2-1* loss-of-function mutant formed large seeds and organs (Figures 1 and 2). Supporting this, the *da2-1* mutation synergistically enhanced the seed and organ size phenotypes of *da1-1* and *da1-ko1* (Figures 1 and 2; see Supplemental Figures 2A to 2D online). The *da2-1* mutation also enhanced the seed and organ size phenotypes of *eod1-2* (see Supplemental Figures 2F and 2G online), further indicating that the *da2-1* mutation promotes seed and organ growth. The *da2-1* mutant formed large ovules with more cells in the integuments, and the *da2-1* mutation synergistically enhanced the ovule size phenotype of *da1-1* (Figures 3H and 3I). In addition, most transgenic plants overexpressing *DA2* and *DA2L* were smaller than wild-type plants (Figures 1F and 1G; see Supplemental Figure 9 online). The organ growth phenotypes of these transgenic plants were correlated with their respective expression levels (see Supplemental Figures 4 and 9 online). Therefore, our data demonstrate that DA2 functions as a negative regulator of seed and organ size. Several *Arabidopsis* mutants with large organs also formed large seeds (Krizek, 1999; Mizukami and Fischer, 2000; Schruff et al., 2006; Li et al., 2008; Adamski et al., 2009), suggesting a possible link between organ size and seed growth. By contrast, several other mutants with large organs exhibited normal sized seeds (Hu et al., 2003; White, 2006; Xu and Li, 2011), indicating that organ and seed size is not invariably positively related. These results suggest that seeds and organs have both common and distinct pathways that regulate their respective size.

Reciprocal cross experiments showed that *DA2* acts maternally to influence seed growth, and the embryo and endosperm genotypes for *DA2* do not affect seed size (Figures 3E to 3G). The integuments surrounding the ovule are maternal tissues and form the seed coat after fertilization. Alterations in maternal integument size, such as those seen in *arf2*, *da1-1*, and *klu* ovules, have been known to contribute to changes in seed size (Schruff et al., 2006; Li et al., 2008; Adamski et al., 2009). Mature *da2-1* ovules were larger than mature wild-type ovules (Figures 3A, 3C, and 3H). The *da2-1* mutation also synergistically enhanced the integument size of *da1-1* ovules (Figures 3A to 3D and 3H). Thus, a general theme emerging from these studies is that the regulation of maternal integument size is a key mechanism in determining final seed size. Consistent with this notion, plant maternal factors of seed size regulation (e.g., KLU, ARF2, and DA1) isolated to date influence integument size (Schruff et al., 2006; Li et al., 2008; Adamski et al., 2009).

The size of the integument or seed coat is determined by cell proliferation and cell expansion, two processes that are coordinated. Cell number in the integuments of the mature ovule sets the growth potential of the seed coat after fertilization. For

example, *arf2* mutants produced large ovules with more cells, leading to large seeds (Schruff et al., 2006), while *klu* mutants had small ovules with fewer cells, resulting in small seeds (Adamski et al., 2009). Our results show that the integuments of *da1-1* and *da2-1* seeds had more cells than those of wild-type seeds, and *da1-1* and *da2-1* act synergistically to promote cell proliferation in the integuments (Figure 3I). We also observed that cells in the outer integuments of *da1-1*, *da2-1*, and *da1-1 da2-1* seeds were shorter than those in wild-type integuments (Figure 3J), suggesting the existence of a possible compensation mechanism between cell proliferation and cell elongation in the maternal integument. Thus, it is possible that the maternal integument or seed coat, which acts as a physical constraint on seed growth, can set an upper limit to final seed size.

A Genetic Framework for Ubiquitin-Mediated Regulation of Seed Size

DA2 encodes a protein with one predicted RING domain that is distinctive from any of the previously described plant RING domains. The RING domain of DA2 shared the highest homology (81.4% identity) with that of rice GW2 (C5HC2), but it lacked one conserved metal ligand amino acid (a His residue) that was replaced by an Asn residue (see Supplemental Figure 4 and Supplemental Data Set 1 online) (Song et al., 2007). It is still possible that the RING domain of DA2 might be a variant of that found in GW2. Many RING-type domains are found in E3 ubiquitin ligases that ubiquitinate substrates, often targeting them for subsequent proteasomal degradation (Smalle and Vierstra, 2004). We tested the E3 activity of recombinant DA2 in an in vitro ubiquitin-ligase assay and demonstrated that DA2 is a functional E3 ubiquitin ligase (Figure 4C), suggesting that DA2 may target positive regulators of cell proliferation for ubiquitin-dependent degradation by the 26S proteasome. Proteins that share homology with DA2 outside the RING domain are found in *Arabidopsis* and other plant species (see Supplemental Data Set 1 and Supplemental Figure 7 online). In *Arabidopsis*, the DA2L protein shares extensive amino acid similarity with DA2 (see Supplemental Data Set 1 online). Like *35S:DA2* plants, *DA2L*-overexpressing lines showed small plants (see Supplemental Figure 8 online), suggesting that *DA2* and *DA2L* may perform similar functions. The homolog of DA2 in rice is the RING-type (C5HC2) protein GW2 (Song et al., 2007), which has been known to act as a negative regulator of seed size. However, the genetic and molecular mechanisms of *GW2* in seed size regulation are largely unknown in rice.

We previously identified DA1, a ubiquitin receptor with ubiquitin binding activity, as a negative regulator of seed size (Li et al., 2008). A modifier screen identified EOD1 (Li et al., 2008), which is allelic to the E3 ubiquitin ligase BB (Disch et al., 2006). Analysis of double *eod1-2 da1-1* mutants revealed synergistic genetic interactions between *DA1* and *EOD1* (Li et al., 2008), suggesting that these genes may control regulate seed growth by modulating the activity of a common target(s). Although genetic interactions between *da1-1* and *eod1-2* also synergistically enhanced seed and organ size, our genetic analyses show that *DA2* acts independently of *EOD1* to influence seed growth, suggesting that DA2 and EOD1 may target distinct growth stimulators for degradation, with common regulation via DA1. Thus, our findings establish a framework for the regulation of seed and organ size by three ubiquitin-related proteins: DA1, DA2, and EOD1. In addition, we observed that overexpression of *GW2* restricts seed and organ growth in *Arabidopsis*, suggesting a possible conserved function in *Arabidopsis* and rice. It would be interesting to investigate the effects of the combination of GW2 and rice homologs of DA1 and EOD1 on grain size in rice.

A Possible Molecular Mechanism of DA1 and DA2 in Seed Size Regulation

Our results demonstrate that the E3 ubiquitin ligase DA2 interacts with the ubiquitin receptor DA1 in vitro and in vivo (Figure 6). However, it is not likely that DA2 targets DA1 for proteasomal degradation because a T-DNA inserted mutant of *DA1* (*da1-ko1*) synergistically enhances the seed size phenotype of *da2-1* (Figures 2D and 2F; see Supplemental Figures 2C and 2D online). Nevertheless, many other types of ubiquitin modification regulate proteins in a proteasome-independent manner (Schnell and Hicke, 2003). For example, monoubiquitination has been implicated in the activation of signaling proteins, endocytosis, and histone modification (Schnell and Hicke, 2003). In animals, monoubiquitination of the ubiquitin receptor eps15 depends on the interaction between eps15 and the Nedd4 family of E3 ligases (Woelk et al., 2006). By contrast, an E3-independent monoubiquitination of ubiquitin receptors has also been reported (Hoeller et al., 2007). Considering that DA1 interacts with DA2, we tested whether DA2 can ubiquitinate or monoubiquitinate DA1. In the presence of E1, E2, and ubiquitin, DA2-His had an E3 ubiquitin ligase activity (see Supplemental Figure 11A online, fifth lane from the left). However, in the presence of E1, E2, ubiquitin, and DA2-His (E3), no ubiquitinated DA1-HA was detected under our reaction conditions (see Supplemental Figure 11B online, sixth lane from the left), suggesting that DA2 might not ubiquitinate DA1.

Ubiquitin receptors can interact with polyubiquitinated substrates of E3s via UIM domains and facilitate their degradation by the proteasome (Verma et al., 2004). We previously demonstrated that UIM domains of DA1 can bind ubiquitin (Li et al., 2008). Taken together with its interaction with DA2 through its C-terminal region (Figures 6A and 6B; see Supplemental Figure 10 online), it is possible that DA1 is involved in mediating the degradation of the ubiquitinated substrates of DA2 by the proteasome. One mechanism may involve an interaction between DA1 and DA2, which helps DA1 specifically recognize the ubiquitinated substrate(s) of DA2. DA1 may subsequently bind the polyubiquitin chains of the ubiquitinated substrate(s) through its UIM domain and mediate the degradation of the ubiquitinated substrate(s).

Improving seed yield is an important target for crop breeders worldwide, and the size of seeds is an important component of overall seed yield. We identified DA2 as an important regulator of seed size that functions synergistically with DA1 to influence seed size. DA1 also acts synergistically with EOD1 to affect seed growth. Overexpression of a dominant-negative *da1-1* mutation (*Zea mays da1-1*) has been reported to increase seed mass of maize (Wang et al., 2012), indicating the promise of combining the effects of

DA1, DA2, and EOD1 from different seed crops to engineer large seed size in these crops.

METHODS

Plant Materials and Growth Conditions

Arabidopsis thaliana ecotype Columbia (Col-0) was the wild-type line used. All mutants were in the Col-0 background. *da2-1* (SALK_150003) was obtained from the Nottingham Arabidopsis Stock Centre and ABRC collections. The T-DNA insertion was confirmed by PCR and sequencing using the primers described in Supplemental Table 1 online. Seeds were surface-sterilized with 100% isopropanol for 1 min and 10% (v/v) household bleach for 10 min, washed at least three times with sterile water, stratified at 4°C for 3 d in the dark, dispersed on GM medium with 0.9% agar and 1% Glc, and then grown at 22°C. Plants were grown under long-day conditions (16-h light/8-h dark) at 22°C.

Constructs and Transformation

The *pDA2*:*DA2* construct was made using a PCR-based Gateway system. The 1960-bp promoter sequence of *DA2* was amplified using the primers DA2proGW-F and DA2proGW-R. PCR products were then cloned into the *pCR8/GW/TOPO TA* cloning vector (Invitrogen). The DA2 coding DNA sequence was amplified using the primers DA2CDSAK-F and DA2CDSAK-R (see Supplemental Table 1 online). PCR products were then cloned into the *Asc*I and *Kpn*I sites of the Gateway vector *pMDC110* to yield the *DA2CDS-pMDC110* plasmid. The *DA2* promoter was then subcloned into *DA2CDS-pMDC110* by the attL × attR reaction to generate the *pDA2:DA2* construct. The plasmid *pDA2*:*DA2* was introduced into *da2-1* mutant plants using *Agrobacterium tumefaciens* GV3101, and transformants were selected on medium containing hygromycin (30 μg/mL).

The 35S:*DA2* construct was made using a PCR-based Gateway system. The specific primers used for the 35S:*DA2* construct are DA2CDS-F and DA2CDS-R (see Supplemental Table 1 online). PCR products were subcloned into the *pCR8/GW/TOPO TA* cloning vector (Invitrogen) using TOPO enzyme. *DA2* was then subcloned into Gateway binary vector *pMDC32* containing the 35S promoter (Curtis and Grossniklaus, 2003). The plasmid *35S*:*DA2* was introduced into Col-0 plants using *Agrobacterium* GV3101, and transformants were selected on medium containing hygromycin (30 μg/mL).

The 1960-bp promoter sequence of *DA2* was amplified using the primers DA2proSN-F and DA2proSN-R (see Supplemental Table 1 online). PCR products were cloned into the *pGEM-T* vector (Promega) using T4 DNA ligase and sequenced. The *DA2* promoter was then inserted into the *Sac*I and *Nco*I sites of the binary vector *pGreen-GUS* (Curtis and Grossniklaus, 2003) to generate the transformation plasmid *pDA2*:*GUS*. The plasmid *pDA2*:*GUS* was introduced into Col-0 plants using *Agrobacterium* GV3101, and transformants were selected on medium containing kanamycin (50 μg/mL).

The *35S*:*GW2* construct was made using a PCR-based Gateway system. The specific primers used for the 35S:*GW2* construct are GW2CDS-F and GW2CDS-R (see Supplemental Table 1 online). PCR products were subcloned into the *pCR8/GW/TOPO TA* cloning vector (Invitrogen) using TOPO enzyme. *GW2* was then subcloned into Gateway binary vector *pMDC32* containing the 35S promoter (Curtis and Grossniklaus, 2003). The plasmid *35S*:*GW2* was introduced into Col-0 plants using *Agrobacterium* GV3101, and transformants were selected on medium containing hygromycin (30 μg/mL).

Morphological and Cellular Analysis

Average seed weight was determined by weighing mature dry seeds in batches of 500 using an electronic analytical balance (Mettler Moledo AL104). The weights of five sample batches were measured for each seed lot. Seeds were photographed under a Leica microscope (S8APO) and a Leica charge-coupled device (DFC420), and seed size was measured using Image J software.

Area measurements of petals (stage 14), leaves, and cotyledons were made by scanning organs to produce a digital image and then calculating area, length, and width using Image J software. Leaf, petal, and embryo cell sizes were measured from differential interference contrast images. Biomass accumulation in flowers (stage 14) was measured by weighing organs.

GUS Staining

Samples (*pDA2*:*GUS*) were stained in a solution of 1 mM 5-bromo-4-chloro-3-indolyl-β-D-glucuronic acid, 100 mM Na_3PO_4 buffer, 3 mM each $K_3Fe(CN)6/K_4Fe(CN)6$, 10 mM EDTA, and 0.1% Nonidet P-40 and incubated at room temperature for 6 h. After GUS staining, chlorophyll was removed using 70% ethanol.

RNA Isolation, RT-PCR, and Quantitative Real-Time RT-PCR Analysis

Total RNA was extracted from *Arabidopsis* roots, stems, leaves, seedlings, and inflorescences using an RNeasy plant mini kit (Tiangen). RT-PCR was performed as described (Li et al., 2006). cDNA samples were standardized based on the amount of *ACTIN2* transcript using the primers ACTIN2-F and ACTIN2-R (see Supplemental Table 1 online). Quantitative real-time RT-PCR analysis was performed with a LightCycler 480 engine (Roche) using the LightCycler 480 SYBR Green Master (Roche). *ACTIN7* mRNA was used as an internal control, and relative amounts of mRNA were calculated using the comparative threshold cycle method. The primers used for RT-PCR and real-time RT-PCR are described in Supplemental Table 1 online.

E3 Ubiquitin Ligase Activity Assay

The coding sequence of *DA2* was cloned into the *Bam*HI and *Pst*I sites of the *pMAL-C2* vector to generate the construct *MBP-DA2*. The specific primers for MBP-DA2 were MBP-DA2-F and MBP-DA2-R (see Supplemental Table 1 online). Mutated DA2 ($DA2^{C59S}$ and $DA2^{N91L}$) was generated by following the instruction manual of a multi-site-directed mutagenesis kit (Stratagene).

Bacterial lysates expressing MBP-DA2 and mutated MBP-DA2 were prepared from *Escherichia coli* BL21 induced with 0.4 mM isopropyl β-D-1-thiogalactopyranoside for 2 h. Bacteria were lysed in Triton Glycerol HEPES lysis buffer (50 mM HEPES, pH 7.5, 150 mM NaCl, 1.5 mM $MgCl_2$, 1 mM EGTA, 1% Triton X-100, 10% glycerol, and protease inhibitor cocktail [Roche]) and sonicated. The lysates were cleared by centrifugation and incubated with amylose resin (New England Biolabs) at 4°C for 30 min. Beads were washed by column buffer (20 mM Tris, pH 7.4, 200 mM NaCl, and 1 mM EDTA) and equilibrated by reaction buffer (50 mM Tris, pH 7.4, 20 mM DTT, 5 mM $MgCl_2$, and 2 mM ATP). Then, 110 ng E1 (Boston Biochem), 170 ng E2 (Boston Biochem), 1 μg His-ubiquitin (Sigma-Aldrich), and 2 μg DA2-MBP or mutated DA2-MBP fusion protein were incubated in a 20-μL reaction buffer for 2 h at 30°C. Polyubiquitinated proteins were detected by immunoblotting with an antibody against His (Abmart) and an antibody against MBP (New England Biolabs).

In Vitro Protein–Protein Interaction

The coding sequences of *DA1*, *da1-1*, and *DA1* derivatives containing specific protein domains were cloned into *Bam*HI and *Not*I sites of the *pGEX-4T-1* vector to generate *GST-DA1*, *GST-DA1*^{R358K}, *GST-DA1-UIM*, and *GST-DA1-LIM+C* constructs, and *Eco*RI and *Xho*I sites of the *pGEX-4T-1* vector to generate *GST-DA1-LIM* and *GST-DA1-C* constructs. The specific primers for *GST-DA1* and *GST-DA1*^{R358K} were GST-DA1-F and

GST-DA1-R (see Supplemental Table 1 online). The specific primers for *GST-DA1-UIM*, *GST-DA1-LIM*, *GST-DA1-LIM+C*, and *GST-DA1-C* were UIM-F, UIM-R, LIM-F, LIM-R, LIM+C-F, LIM+C-R, C-F, and C-R, respectively (see Supplemental Table 1 online).

To test protein–protein interaction, bacterial lysates containing ~15 μg of MBP-DA2 fusion proteins were combined with lysates containing ~30 μg of GST-DA1, GST-DA1^{R358K}, GST-DA1-UIM, GST-DA1-LIM, GST-DA1-LIM+C, or GST-DA1-C fusion proteins. Twenty microliters of amylose resin (New England Biolabs) was added into each combined solution with continued rocking at 4°C for 1 h. Beads were washed five times with TGH buffer, and the isolated proteins were separated on a 10% SDS-polyacrylamide gel and detected by immunoblot analysis with anti-GST (Abmart) and anti-MBP antibodies (Abmart), respectively.

Coimmunoprecipitation

The coding sequence of *DA1* and *DA1-C* was cloned into the *Kpn*I and *Bam*HI sites of the *pCAMBIA1300-221-Myc* vector to generate the transformation plasmid *35S:Myc-DA1* and *35S:Myc-DA1-C*. The specific primers used to amplify *Myc-DA1* and *Myc-DA1-C* were Myc-DA1-F, Myc-DA1-R, Myc-DA1-C-F, and Myc-DA1-C-R, respectively (see Supplemental Table 1 online). The specific primers used to amplify *35S:GFP-DA2* were DA2CDS-F and DA2CDS-R (see Supplemental Table 1 online). PCR products were subcloned into the *pCR8/GW/TOPO TA* cloning vector (Invitrogen) using TOPO enzyme. *DA2* was then subcloned into Gateway binary vector *pMDC43* containing the 35S promoter and *GFP* (Curtis and Grossniklaus, 2003). The specific primers used for the *35S:PEX10-GFP* construct are PEX10-F and PEX10-R (see Supplemental Table 1 online). PCR products were subcloned into the *pCR8/GW/TOPO TA* cloning vector (Invitrogen) using TOPO enzyme. *PEX10* was then subcloned into Gateway binary vector *pH7FWG2* containing the 35S promoter and *GFP*.

Nicotiana benthamiana leaves were transformed by injection of *Agrobacterium* GV3101 cells harboring *35S:Myc-DA1* and *35S:GFP-DA2* plasmids as previously described (Voinnet et al., 2003). Total protein was extracted with extraction buffer (50 mM Tris/HCl, pH 7.5, 150 mM NaCl, 20% glycerol, 2% Triton X-100, 1 mM EDTA, 1× Complete protease inhibitor cocktail [Roche], and 20 μg/mL MG132) and incubated with GFP-Trap-A (Chromotek) for 1 h at 4°C. Beads were washed three times with wash buffer (50 mM Tris/HCl, pH 7.5, 150 mM NaCl, 0.1% Triton X-100, and 1× Complete protease inhibitor cocktail [Roche]). The immunoprecipitates were separated in 10% SDS-polyacrylamide gel and detected by immunoblot analysis with anti-GFP (Beyotime) and anti-Myc (Abmart) antibodies, respectively.

Accession Numbers

Arabidopsis Genome Initiative locus identifiers for genes mentioned in this article are as follows: At1g19270 (*DA1*), At4g36860 (*DAR1*), At1g78420 (*DA2*), At1g17145 (*DA2L*), and At3g63530 (*EOD1/BB*). Other sequence data from this article can be found in the Arabidopsis Genome Initiative or GenBank/EMBL databases under the following accession numbers: Os_GW2 (ABO31101.1), Bd_Bradi3g09270 (XP_003571977), Hv_Yrg1 (ABY51682), Zm_gi|220961719 (ACL93316), Sb_gi|242064618 (XP_002453598), At_DA2 (NP_565180), At_DA2L (NP_564016), Rc_gi|255578534 (XP_002530130), Pt_gi|224061326 (XP_002300427), Vv_DA2 (CAN66658), Gm_Glyma13g33260.1 (XP_003543150), Sb_Sb10g003820 (XP_002436503), Zm_gi|260935347 (ACX54355), Os_gi|218197613 (EEC80040), and Bd_Bradi1g49080 (XP_003564311).

Supplemental Data

The following materials are available in the online version of this article.

Supplemental Figure 1. Organ Size in the *da2-1* Mutant.

Supplemental Figure 2. *DA1* and *DA2* Act Synergistically to Regulate Seed Size.

Supplemental Figure 3. Molecular Characterization of the *DA2* Gene.

Supplemental Figure 4. Overexpression of *DA2* Restricts Organ Growth.

Supplemental Figure 5. Alignment of RING Domain of DA2 Homologs.

Supplemental Figure 6. The Seed Size Phenotype of *35S:DA2^{C59S}* and *35S:DA2^{N91L}*.

Supplemental Figure 7. Phylogenetic Tree of DA2 Homologs.

Supplemental Figure 8. Overexpression of *DA2L* Restricts Organ Growth.

Supplemental Figure 9. Overexpression of *GW2* Restricts Seed and Organ Growth.

Supplemental Figure 10. The C-Terminal Region of DA1 Interacts with DA2 in Planta.

Supplemental Figure 11. DA2 Has E3 Ubiquitin Ligase Activity, but May Not Ubiquitinate DA1.

Supplemental Table 1. Primers Used in This Study.

Supplemental Data Set 1. Alignment of DA2 Homologs Used to Generate Phylogeny Presented in Supplemental Figure 7 Online.

ACKNOWLEDGMENTS

We thank the anonymous reviewers and the editor for their critical comments on this article, Qi Xie for his suggestions on ubiquitination assay, and the ABRC and the Nottingham Arabidopsis Stock Centre for the *da2-1* mutant. This work was supported by the National Basic Research Program of China (2009CB941503) and National Natural Science Foundation of China (31300242, 91017014, 31221063, and 30870215).

AUTHOR CONTRIBUTIONS

T.X., N.L., and Y.L. designed the research. T.X., N.L., J.L., and F.G. performed most of the experiments. N.L. and J.L. detected the E3 ubiquitin activity of DA2. J.D. and A.K. performed the DA1 ubiquitination assay. T.X., N.L., M.W.B., and Y.L. analyzed the data. T.X., N.L., and Y.L. wrote the article.

Received June 18, 2013; revised August 9, 2013; accepted August 27, 2013; published September 17, 2013.

REFERENCES

Adamski, N.M., Anastasiou, E., Eriksson, S., O'Neill, C.M., and Lenhard, M. (2009). Local maternal control of seed size by KLUH/CYP78A5-dependent growth signaling. Proc. Natl. Acad. Sci. USA **106:** 20115–20120.

Alexandru, G., Graumann, J., Smith, G.T., Kolawa, N.J., Fang, R., and Deshaies, R.J. (2008). UBXD7 binds multiple ubiquitin ligases and implicates p97 in HIF1alpha turnover. Cell **134:** 804–816.

Alonso-Blanco, C., Blankestijn-de Vries, H., Hanhart, C.J., and Koornneef, M. (1999). Natural allelic variation at seed size loci in relation to other life history traits of *Arabidopsis thaliana*. Proc. Natl. Acad. Sci. USA **96:** 4710–4717.

Bandau, S., Knebel, A., Gage, Z.O., Wood, N.T., and Alexandru, G. (2012). UBXN7 docks on neddylated cullin complexes using its UIM motif and causes HIF1α accumulation. BMC Biol. **10:** 36.

Curtis, M.D., and Grossniklaus, U. (2003). A Gateway cloning vector set for high-throughput functional analysis of genes in planta. Plant Physiol. **133:** 462–469.

Disch, S., Anastasiou, E., Sharma, V.K., Laux, T., Fletcher, J.C., and Lenhard, M. (2006). The E3 ubiquitin ligase BIG BROTHER controls *Arabidopsis* organ size in a dosage-dependent manner. Curr. Biol. **16:** 272–279.

Fan, C., Xing, Y., Mao, H., Lu, T., Han, B., Xu, C., Li, X., and Zhang, Q. (2006). GS3, a major QTL for grain length and weight and minor QTL for grain width and thickness in rice, encodes a putative transmembrane protein. Theor. Appl. Genet. **112:** 1164–1171.

Fang, W., Wang, Z., Cui, R., Li, J., and Li, Y. (2012). Maternal control of seed size by EOD3/CYP78A6 in *Arabidopsis thaliana*. Plant J. **70:** 929–939.

Garcia, D., Fitz Gerald, J.N., and Berger, F. (2005). Maternal control of integument cell elongation and zygotic control of endosperm growth are coordinated to determine seed size in *Arabidopsis*. Plant Cell **17:** 52–60.

Garcia, D., Saingery, V., Chambrier, P., Mayer, U., Jürgens, G., and Berger, F. (2003). Arabidopsis haiku mutants reveal new controls of seed size by endosperm. Plant Physiol. **131:** 1661–1670.

Gegas, V.C., Nazari, A., Griffiths, S., Simmonds, J., Fish, L., Orford, S., Sayers, L., Doonan, J.H., and Snape, J.W. (2010). A genetic framework for grain size and shape variation in wheat. Plant Cell **22:** 1046–1056.

Gómez, J.M. (2004). Bigger is not always better: Conflicting selective pressures on seed size in *Quercus ilex*. Evolution **58:** 71–80.

Hoeller, D., Hecker, C.M., Wagner, S., Rogov, V., Dötsch, V., and Dikic, I. (2007). E3-independent monoubiquitination of ubiquitin-binding proteins. Mol. Cell **26:** 891–898.

Hu, Y., Xie, Q., and Chua, N.H. (2003). The *Arabidopsis* auxin-inducible gene ARGOS controls lateral organ size. Plant Cell **15:** 1951–1961.

Jofuku, K.D., Omidyar, P.K., Gee, Z., and Okamuro, J.K. (2005). Control of seed mass and seed yield by the floral homeotic gene APETALA2. Proc. Natl. Acad. Sci. USA **102:** 3117–3122.

Kaur, N., Zhao, Q., Xie, Q., and Hu, J. (2013). *Arabidopsis* RING peroxins are E3 ubiquitin ligases that interact with two homologous ubiquitin receptor proteins(F). J. Integr. Plant Biol. **55:** 108–120.

Krizek, B.A. (1999). Ectopic expression of AINTEGUMENTA in *Arabidopsis* plants results in increased growth of floral organs. Dev. Genet. **25:** 224–236.

Lanctot, A.A., Peng, C.Y., Pawlisz, A.S., Joksimovic, M., and Feng, Y. (2013). Spatially dependent dynamic MAPK modulation by the Nde1-Lis1-Brap complex patterns mammalian CNS. Dev. Cell **25:** 241–255.

Li, Y., Lee, K.K., Walsh, S., Smith, C., Hadingham, S., Sorefan, K., Cawley, G., and Bevan, M.W. (2006). Establishing glucose- and ABA-regulated transcription networks in *Arabidopsis* by microarray analysis and promoter classification using a Relevance Vector Machine. Genome Res. **16:** 414–427.

Li, Y., Zheng, L., Corke, F., Smith, C., and Bevan, M.W. (2008). Control of final seed and organ size by the DA1 gene family in *Arabidopsis thaliana*. Genes Dev. **22:** 1331–1336.

Lopes, M.A., and Larkins, B.A. (1993). Endosperm origin, development, and function. Plant Cell **5:** 1383–1399.

Luo, M., Dennis, E.S., Berger, F., Peacock, W.J., and Chaudhury, A. (2005). MINISEED3 (MINI3), a WRKY family gene, and HAIKU2 (IKU2), a leucine-rich repeat (LRR) KINASE gene, are regulators of seed size in *Arabidopsis*. Proc. Natl. Acad. Sci. USA **102:** 17531–17536.

Mizukami, Y., and Fischer, R.L. (2000). Plant organ size control: AINTEGUMENTA regulates growth and cell numbers during organogenesis. Proc. Natl. Acad. Sci. USA **97:** 942–947.

Moles, A.T., Ackerly, D.D., Webb, C.O., Tweddle, J.C., Dickie, J.B., and Westoby, M. (2005). A brief history of seed size. Science **307:** 576–580.

Ohto, M.A., Fischer, R.L., Goldberg, R.B., Nakamura, K., and Harada, J.J. (2005). Control of seed mass by APETALA2. Proc. Natl. Acad. Sci. USA **102:** 3123–3128.

Ohto, M.A., Floyd, S.K., Fischer, R.L., Goldberg, R.B., and Harada, J.J. (2009). Effects of APETALA2 on embryo, endosperm, and seed coat development determine seed size in *Arabidopsis*. Sex. Plant Reprod. **22:** 277–289.

Orsi, C.H., and Tanksley, S.D. (2009). Natural variation in an ABC transporter gene associated with seed size evolution in tomato species. PLoS Genet. **5:** e1000347.

Pérez-Pérez, J.M., Candela, H., and Micol, J.L. (2009). Understanding synergy in genetic interactions. Trends Genet. **25:** 368–376.

Platta, H.W., El Magraoui, F., Bäumer, B.E., Schlee, D., Girzalsky, W., and Erdmann, R. (2009). Pex2 and pex12 function as protein-ubiquitin ligases in peroxisomal protein import. Mol. Cell. Biol. **29:** 5505–5516.

Schnell, J.D., and Hicke, L. (2003). Non-traditional functions of ubiquitin and ubiquitin-binding proteins. J. Biol. Chem. **278:** 35857–35860.

Schruff, M.C., Spielman, M., Tiwari, S., Adams, S., Fenby, N., and Scott, R.J. (2006). The AUXIN RESPONSE FACTOR 2 gene of *Arabidopsis* links auxin signalling, cell division, and the size of seeds and other organs. Development **133:** 251–261.

Seo, H.S., Yang, J.Y., Ishikawa, M., Bolle, C., Ballesteros, M.L., and Chua, N.H. (2003). LAF1 ubiquitination by COP1 controls photomorphogenesis and is stimulated by SPA1. Nature **423:** 995–999.

Shomura, A., Izawa, T., Ebana, K., Ebitani, T., Kanegae, H., Konishi, S., and Yano, M. (2008). Deletion in a gene associated with grain size increased yields during rice domestication. Nat. Genet. **40:** 1023–1028.

Smalle, J., and Vierstra, R.D. (2004). The ubiquitin 26S proteasome proteolytic pathway. Annu. Rev. Plant Biol. **55:** 555–590.

Song, X.J., Huang, W., Shi, M., Zhu, M.Z., and Lin, H.X. (2007). A QTL for rice grain width and weight encodes a previously unknown RING-type E3 ubiquitin ligase. Nat. Genet. **39:** 623–630.

Stone, S.L., Hauksdóttir, H., Troy, A., Herschleb, J., Kraft, E., and Callis, J. (2005). Functional analysis of the RING-type ubiquitin ligase family of *Arabidopsis*. Plant Physiol. **137:** 13–30.

Van Daele, I., Gonzalez, N., Vercauteren, I., de Smet, L., Inzé, D., Roldán-Ruiz, I., and Vuylsteke, M. (2012). A comparative study of seed yield parameters in *Arabidopsis thaliana* mutants and transgenics. Plant Biotechnol. J. **10:** 488–500.

Verma, R., Oania, R., Graumann, J., and Deshaies, R.J. (2004). Multiubiquitin chain receptors define a layer of substrate selectivity in the ubiquitin-proteasome system. Cell **118:** 99–110.

Voinnet, O., Rivas, S., Mestre, P., and Baulcombe, D. (2003). An enhanced transient expression system in plants based on suppression of gene silencing by the p19 protein of tomato bushy stunt virus. Plant J. **33:** 949–956.

Wang, A., Garcia, D., Zhang, H., Feng, K., Chaudhury, A., Berger, F., Peacock, W.J., Dennis, E.S., and Luo, M. (2010). The VQ motif protein IKU1 regulates endosperm growth and seed size in *Arabidopsis*. Plant J. **63:** 670–679.

Wang, X., Liu, B., Huang, C., Zhang, X., Luo, C., Cheng, X., Yu, R., and Wu, Z. (2012). Over expression of Zmda1-1 gene increases seed mass of corn. Afr. J. Biotechnol. **11:** 13387–13395.

Weng, J., et al. (2008). Isolation and initial characterization of GW5, a major QTL associated with rice grain width and weight. Cell Res. **18:** 1199–1209.

Westoby, M., Falster, D.S., Moles, A.T., Vesk, P.A., and Wright, I.J. (2002). PLANT ECOLOGICAL STRATEGIES: Some leading dimensions of variation between species. Annu. Rev. Ecol. Syst. **33:** 125–159.

White, D.W. (2006). PEAPOD regulates lamina size and curvature in *Arabidopsis*. Proc. Natl. Acad. Sci. USA **103:** 13238–13243.

Woelk, T., Oldrini, B., Maspero, E., Confalonieri, S., Cavallaro, E., Di Fiore, P.P., and Polo, S. (2006). Molecular mechanisms of coupled monoubiquitination. Nat. Cell Biol. **8:** 1246–1254.

Xie, Q., Guo, H.S., Dallman, G., Fang, S., Weissman, A.M., and Chua, N.H. (2002). SINAT5 promotes ubiquitin-related degradation of NAC1 to attenuate auxin signals. Nature **419:** 167–170.

Xu, R., and Li, Y. (2011). Control of final organ size by Mediator complex subunit 25 in *Arabidopsis thaliana*. Development **138:** 4545–4554.

Zhou, Y., Zhang, X., Kang, X., Zhao, X., Zhang, X., and Ni, M. (2009). SHORT HYPOCOTYL UNDER BLUE1 associates with MINISEED3 and HAIKU2 promoters in vivo to regulate *Arabidopsis* seed development. Plant Cell **21:** 106–117.